

Thermal Effects on Neutrino–Nucleus Inelastic Scattering in Stellar Environments

A. A. Dzhioev^{1)**}, A. I. Vdovin^{1)***}, V. Yu. Ponomarev^{2)****}, and J. Wambach^{2),3)*****}

Received December 6, 2010

Abstract—Thermal effects for inelastic neutrino–nucleus scattering off even–even nuclei in the iron region are studied. Allowed and first-forbidden contributions to the cross sections are calculated within the quasiparticle random-phase approximation, extended to finite temperatures within the Thermo-Field-Dynamics formalism. The GT_0 strength distribution at finite temperatures is calculated for the sample nucleus ^{54}Fe . The neutral-current neutrino–nucleus inelastic cross section is calculated for relevant temperatures during the supernova core collapse. The thermal population of the excited states significantly enhances the cross section at low neutrino energies. In agreement with studies using a large scale shell-model approach the enhancement is mainly due to neutrino up-scattering at finite temperatures.

DOI: 10.1134/S1063778811080059

1. INTRODUCTION

Neutrinos play a decisive role in core-collapse supernova explosions since they carry most of the gravitational binding energy released. The transport of neutrinos through the hot and dense stellar environment is believed to ultimately be responsible for a successful explosion, although the details are not fully understood yet. The present paper addresses the role of thermal effects in the inelastic neutrino–nucleus scattering in the iron core during infall and shortly after bounce.

At the end of the 1980th it was pointed out by Haxton that inelastic neutrino–nucleus scattering (INNS) mediated by the neutral current can be of importance comparable with the other processes of neutrino down-scattering [1]. The INNS contributes to the neutrino opacities and thermalization during the collapse phase, the revival of the stalled shock wave in the delayed explosion mechanism, and to explosive nucleosynthesis. The estimates by Haxton were based on nuclei in their respective ground states, i.e. for a “cold” nuclei. Subsequently, it was realized that the INNS occurs in hot stellar environment

($T \geq 0.8$ MeV) and, due to the thermal population of nuclear excited states, sizeable changes of the INNS cross section are to be expected. The effect was firstly analyzed in [2] and then in [3] on the basis of large-scale shell-model (LSSM) calculations. In [3, 4], it was found that the INNS cross section noticeably increases at $T \neq 0$ and for neutrino energies $E_\nu \lesssim 10$ MeV, especially for neutrino scattering off even–even nuclides.

However, in the subsequent core-collapse supernova simulations [5] including several dozens of nuclides, it was demonstrated that the inclusion of the INNS process does not have a large effect on the collapse dynamics and the shock wave propagation. But it significantly modifies the spectrum of neutrinos generated in the ν_e burst.

Here, we apply an alternative approach for treating the thermal effects for INNS cross sections. In essence, our approach is based on the thermal quasiparticle random-phase approximation (TQRPA). We apply it in the context of thermo-field-dynamics (TFD), which enables a transparent treatment of thermal excitation and de-excitation processes and offers the possibility for systematic improvements. This approach has recently been used in studies of the electron capture on hot iron and germanium nuclei under stellar conditions [6].

2. FORMALISM

2.1. Fundamentals of the Thermo-Field-Dynamics

Thermo-field-dynamics [7–9] is a real-time formalism for treating thermal effects in quantum field

*The text was submitted by the authors in English.

¹⁾Bogoliubov Laboratory of Theoretical Physics, JINR, Dubna, Russia.

²⁾Institute for Nuclear Physics, TU Darmstadt, Germany.

³⁾GSI, Darmstadt, Germany.

**E-mail: dzhioev@theor.jinr.ru

***E-mail: vdovin@theor.jinr.ru

****E-mail: ponomare@crunch.ikp.physik.tu-darmstadt.de

*****E-mail: Jochen.Wambach@physik.tu-darmstadt.de

theory and nonrelativistic many-body theories. The standard TFD formalism treats a many-body system in thermal equilibrium with a heat bath and a particle reservoir in the grand canonical ensemble. The thermal average of a given operator A is calculated as the expectation value in a specially constructed, temperature-dependent state $|0(T)\rangle$ which is termed the thermal vacuum. This expectation value is equal to the usual grand canonical average of A . In this sense, the thermal vacuum describes the hot system in the thermal equilibrium.

To construct the state $|0(T)\rangle$, a formal doubling of the system degrees of freedom is introduced. In TFD, a tilde conjugate operator \tilde{A} —acting in the independent Hilbert space—is associated with A , in accordance with properly formulated tilde conjugation rules [7–9]. For a system governed by the Hamiltonian H at $T = 0$, the whole Hilbert space at $T \neq 0$ is spanned by the direct product of the eigenstates of H ($H|n\rangle = E_n|n\rangle$) and those of the tilde Hamiltonian \tilde{H} having the same eigenvalues ($\tilde{H}|\tilde{n}\rangle = E_n|\tilde{n}\rangle$). The important point is that, in the doubled Hilbert space, the time-translation operator is not the initial Hamiltonian H , but instead the thermal Hamiltonian $\mathcal{H} = H - \tilde{H}$. This implies that the excitations of the thermal system are obtained by the diagonalization of \mathcal{H} .

The thermal vacuum is the zero-energy eigenstate of the thermal Hamiltonian \mathcal{H} and satisfies the thermal state condition [7–9]

$$A|0(T)\rangle = \sigma e^{\mathcal{H}/2T} \tilde{A}^\dagger |0(T)\rangle, \quad (1)$$

where $\sigma = 1$ for bosonic A and $\sigma = i$ for fermionic A .

As it follows from the definition of \mathcal{H} , each of its eigenstates with positive energy has the counterpart—the tilde-conjugate eigenstate—with negative but the same absolute energy value. This allows to treat excitation and de-excitation processes at finite temperatures.

Obviously, in most practical cases one cannot diagonalize \mathcal{H} exactly. Usually, one resorts to certain approximations such as Hartree–Fock–Bogoliubov (HFB) mean-field theory and the random-phase approximation (RPA) (see, e.g., [10]). In what follows the TFD studies for neutrino-induced charge-neutral excitations in hot nuclei are based in part on the results of [11, 12] (see also [6]).

2.2. Charge-Neutral Excitations in Hot Nuclei

In what follows we employ the Hamiltonian of the quasiparticle–phonon model (QPM) H_{QPM} [13] which consists of proton and neutron mean fields H_{sp} , the BCS pairing interactions H_{pair} and isoscalar

and isovector separable particle–hole interactions. Since the INNS involves nuclear J^π excitations of both natural ($\pi = (-1)^J$) and unnatural ($\pi = (-1)^{J+1}$) parities both the separable multipole H_{M}^{ph} and spin-multipole $H_{\text{SM}}^{\text{ph}}$ interactions are included in the particle–hole channel

$$H_{\text{QPM}} = H_{\text{sp}} + H_{\text{pair}} + H_{\text{M}}^{\text{ph}} + H_{\text{SM}}^{\text{ph}}. \quad (2)$$

The four terms of H_{QPM} read

$$\begin{aligned} H_{\text{sp}} &= \sum_{\tau=p,n} \sum_{jm}^\tau (E_j - \lambda_\tau) a_{jm}^\dagger a_{jm}, \\ H_{\text{pair}} &= -\frac{1}{4} \sum_{\tau=p,n} G_\tau \sum_{\substack{jm \\ j'm'}}^\tau a_{jm}^\dagger a_{j\bar{m}}^\dagger a_{j'm'} a_{j'\bar{m}'}, \\ H_{\text{M}}^{\text{ph}} &= -\frac{1}{2} \sum_{\lambda\mu} \sum_{\tau\rho=\pm 1} (\kappa_0^{(\lambda)} \\ &\quad + \rho\kappa_1^{(\lambda)}) M_{\lambda\mu}^+(\tau) M_{\lambda\mu}(\rho\tau), \\ H_{\text{SM}}^{\text{ph}} &= -\frac{1}{2} \sum_{L\lambda\mu} \sum_{\tau\rho=\pm 1} (\kappa_0^{(L\lambda)} \\ &\quad + \rho\kappa_1^{(L\lambda)}) S_{L\lambda\mu}^+(\tau) S_{L\lambda\mu}(\rho\tau). \end{aligned}$$

Here, we use standard notation of the QPM. Namely, a_{jm}^\dagger and a_{jm} are the creation and annihilation operators of particle with quantum numbers $jm \equiv n, l, j, m$ and energy E_j ; $\bar{j}\bar{m}$ stands for the time-reversed single-particle states; the index τ is isotopic one and changing the sign of τ means changing $n \leftrightarrow p$; the parameter G_τ is the constant of pairing interaction; λ_τ is the chemical potential; the parameters $\kappa_0^{(a)}$ ($\kappa_1^{(a)}$) denote the strength parameters of the isoscalar (isovector) multipole ($a \equiv \lambda$ is a multipole index) and spin-multipole ($a \equiv L\lambda$ is a spin-multipole index) forces. The multipole $M_{\lambda\mu}^+(\tau)$ and spin-multipole $S_{L\lambda\mu}^+(\tau)$ single-particle operators read as

$$\begin{aligned} M_{\lambda\mu}^+(\tau) &= \sum_{\substack{j_1 m_1 \\ j_2 m_2}}^\tau \langle j_1 m_1 | i^\lambda R_\lambda(r) Y_{\lambda\mu} | \\ &\quad \times j_2 m_2 \rangle a_{j_1 m_1}^\dagger a_{j_2 m_2}, \\ S_{L\lambda\mu}^+(\tau) &= \sum_{\substack{j_1 m_1 \\ j_2 m_2}}^\tau \langle j_1 m_1 | i^L R_L(r) [Y_L \sigma]_\mu^\lambda | \\ &\quad \times j_2 m_2 \rangle a_{j_1 m_1}^\dagger a_{j_2 m_2}, \end{aligned} \quad (3)$$

where

$$[Y_L \sigma]_\mu^\lambda = \sum_{M,m} \langle LM1m | \lambda\mu \rangle Y_{LM}(\theta, \phi) \sigma_m,$$

and the notation \sum^τ implies a summation over neutron ($\tau = n$) or proton ($\tau = p$) single-particle states only. The excitations of natural parity are generated by the multipole and spin-multipole $L = \lambda$ interactions, while the spin-multipole interactions with $L = \lambda \pm 1$ are responsible for the states of unnatural parity.

To determine the thermal behavior of a nucleus governed by the Hamiltonian (2) we should diagonalize the thermal Hamiltonian $\mathcal{H}_{\text{QPM}} = H_{\text{QPM}} - \tilde{H}_{\text{QPM}}$ and find the corresponding thermal vacuum state. This will be done in two steps.

In a first step, the sum of single-particle and pairing terms $\mathcal{H}_{\text{BCS}} = \mathcal{H}_{\text{sp}} + \mathcal{H}_{\text{pair}}$ is diagonalized. To this end, two subsequent unitary transformations are made. The first is the usual Bogoliubov u, v transformation from the original particle operators a_{jm}^\dagger, a_{jm} to the quasiparticle ones $\alpha_{jm}^\dagger, \alpha_{jm}$. The same transformation is applied to the tilde operators $\tilde{a}_{jm}^\dagger, \tilde{a}_{jm}$, thus producing the tilde quasiparticle operators $\tilde{\alpha}_{jm}^\dagger, \tilde{\alpha}_{jm}$. The second, unitary thermal Bogoliubov transformation mixes the original and tilde degrees of freedom

$$\begin{aligned}\beta_{jm}^\dagger &= x_j \alpha_{jm}^\dagger - iy_j \tilde{\alpha}_{jm}, \\ \tilde{\beta}_{jm}^\dagger &= x_j \tilde{\alpha}_{jm}^\dagger + iy_j \alpha_{jm} \quad (x_j^2 + y_j^2 = 1).\end{aligned}\quad (4)$$

The operators $\beta_{jm}^\dagger, \beta_{jm}, \tilde{\beta}_{jm}^\dagger$, and $\tilde{\beta}_{jm}$ are called thermal quasiparticle operators.

The coefficients u_j, v_j, x_j, y_j are found by diagonalizing \mathcal{H}_{BCS} and demanding that the vacuum of thermal quasiparticles is the thermal vacuum in the BCS approximation, i.e., it obeys the thermal state condition (1). As a result, one obtains the following equations for u_j, v_j and x_j, y_j :

$$\begin{aligned}v_j &= \frac{1}{\sqrt{2}} \left(1 - \frac{E_j - \lambda_\tau}{\varepsilon_j} \right)^{1/2}, \\ u_j &= (1 - v_j^2)^{1/2},\end{aligned}\quad (5)$$

$$y_j = \left[1 + \exp\left(\frac{\varepsilon_j}{T}\right) \right]^{-1/2}, \quad x_j = (1 - y_j^2)^{1/2}, \quad (6)$$

where $\varepsilon_j = \sqrt{(E_j - \lambda_\tau)^2 + \Delta_\tau^2}$. The coefficients y_j^2 determine the average number of thermally excited Bogoliubov quasiparticles in the BCS thermal vacuum

$$\langle 0(T); \text{qp} | \alpha_{jm}^\dagger \alpha_{jm} | 0(T); \text{qp} \rangle = y_j^2 \quad (7)$$

and, thus, coincide with the thermal occupation factors of the Fermi–Dirac statistics.

The pairing gap Δ_τ and the chemical potential λ_τ are the solutions to the finite-temperature BCS equations

$$\begin{aligned}\Delta_\tau(T) &= \frac{G_\tau}{2} \sum_j^\tau (2j+1)(1 - 2y_j^2)u_j v_j, \\ N_\tau &= \sum_j^\tau (2j+1)(v_j^2 x_j^2 + u_j^2 y_j^2),\end{aligned}\quad (8)$$

where N_τ is the number of neutrons or protons in a nucleus.

At this stage, the thermal BCS Hamiltonian \mathcal{H}_{BCS} is diagonal

$$\mathcal{H}_{\text{BCS}} \simeq \sum_\tau \sum_{jm}^\tau \varepsilon_j(T) (\beta_{jm}^\dagger \beta_{jm} - \tilde{\beta}_{jm}^\dagger \tilde{\beta}_{jm})$$

and corresponds to a system of noninteracting thermal quasiparticles. The vacuum for thermal quasiparticles $|0(T); \text{qp}\rangle$ is the thermal vacuum in the BCS approximation. The states $\beta_{jm}^\dagger |0(T); \text{qp}\rangle$ have positive excitation energies, whereas the corresponding tilde-states $\tilde{\beta}_{jm}^\dagger |0(T); \text{qp}\rangle$ have negative energies. Since the thermal vacuum contains a certain number of Bogoliubov quasiparticles, excited states can be built on $|0(T); \text{qp}\rangle$ by either adding or removing a Bogoliubov quasiparticle. The first process corresponds to the creation of a non-tilde thermal quasiparticle with positive energy, whereas the second process creates a tilde quasiparticle with negative energy.

At the second step of the approximate diagonalization of \mathcal{H}_{QPM} , long-range correlations due to the particle–hole interaction are taken into account within the TQRPA. Within the TFD formalism the terms $\mathcal{H}_M^{\text{ph}}$ and $\mathcal{H}_{\text{SM}}^{\text{ph}}$ are written in terms of the thermal quasiparticle operators determined above. Then, \mathcal{H}_{QPM} is approximately diagonalized within a basis of thermal phonon operators

$$\begin{aligned}Q_{\lambda\mu}^\dagger &= \frac{1}{2} \sum_\tau \sum_{j_1 j_2}^\tau \left\{ \psi_{j_1 j_2}^{\lambda i} [\beta_{j_1}^\dagger \beta_{j_2}^\dagger]_\mu^\lambda \right. \\ &+ \tilde{\psi}_{j_1 j_2}^{\lambda i} [\tilde{\beta}_{j_1}^\dagger \tilde{\beta}_{j_2}^\dagger]_\mu^\lambda + 2i\eta_{j_1 j_2}^{\lambda i} [\beta_{j_1}^\dagger \tilde{\beta}_{j_2}^\dagger]_\mu^\lambda \\ &+ \phi_{j_1 j_2}^{\lambda i} [\beta_{j_1} \beta_{j_2}]_\mu^\lambda + \tilde{\phi}_{j_1 j_2}^{\lambda i} [\tilde{\beta}_{j_1} \tilde{\beta}_{j_2}]_\mu^\lambda \\ &\left. + 2i\xi_{j_1 j_2}^{\lambda i} [\beta_{j_1} \tilde{\beta}_{j_2}]_\mu^\lambda \right\},\end{aligned}\quad (9)$$

where $[\]_\mu^\lambda$ denotes the coupling of single-particle angular momenta j_1, j_2 to a total angular momentum λ . Now the thermal equilibrium state is treated as the vacuum $|0(T); \text{ph}\rangle$ for the thermal phonon annihilation operators.

The thermal phonon operators are considered as bosonic ones which imposes certain constraint on the phonon amplitudes. To find the amplitudes and

energies of the thermal phonons, the variational principle is used, i.e., we find the minimum of the average value of thermal Hamiltonian with respect to the one-phonon states $Q_{\lambda\mu i}^\dagger|0(T); \text{ph}\rangle$ or $\tilde{Q}_{\lambda\mu i}^\dagger|0(T); \text{ph}\rangle$ under the aforementioned constraint.

After variation one obtains a system of linear equations for the amplitudes $\psi_{j_1 j_2}^{\lambda i}$, $\tilde{\psi}_{j_1 j_2}^{\lambda i}$, $\eta_{j_1 j_2}^{\lambda i}$, etc. as well as for the energies (details can be found in [11]). These constitute the equations for the TQRPA. In contrast to the zero temperature case, the negative solutions of the secular equation have a physical meaning. They correspond to the tilde thermal one-phonon states and arise from $\tilde{\beta}^\dagger \tilde{\beta}^\dagger$ terms in the thermal phonon operator. As it was noted above, creation of a tilde thermal quasiparticle corresponds to the annihilation of a thermally excited Bogoliubov quasiparticle. Consequently, excitations of negative-energy thermal phonons correspond to transitions from thermally excited nuclear states.

After diagonalization in terms of thermal phonon operators the TQRPA part of the \mathcal{H}_{QPM} takes the form

$$\mathcal{H}_{\text{TRPA}} = \sum_{\lambda\mu i} \omega_{\lambda i} (Q_{\lambda\mu i}^\dagger Q_{\lambda\mu i} - \tilde{Q}_{\lambda\mu i}^\dagger \tilde{Q}_{\lambda\mu i}). \quad (10)$$

To fix properly the thermal vacuum state $|0(T); \text{ph}\rangle$ corresponding to TRPA we once again turn to the thermal state condition (1) and derive the final expressions for the amplitudes of the thermal phonon operator (9).

Once the structure of thermal phonons is determined, one can determine the transition probabilities from the thermal vacuum to thermal one-phonon states. They are given by the squared reduced matrix elements of the corresponding transition operator $\mathcal{T}_{\lambda\mu}$

$$\begin{aligned} \Phi_{\lambda i} &= |\langle Q_{\lambda i} | \mathcal{T}_\lambda | 0(T); \text{ph} \rangle|^2, \\ \tilde{\Phi}_{\lambda i} &= |\langle \tilde{Q}_{\lambda i} | \mathcal{T}_\lambda | 0(T); \text{ph} \rangle|^2. \end{aligned} \quad (11)$$

Thus, the probability to excite the hot nucleus is given by $\Phi_{\lambda i}$, while $\tilde{\Phi}_{\lambda i}$ is the probability to de-excite it.

2.3. Cross Section of Inelastic Neutrino–Nucleus Scattering

Considering INNS in stellar environments we assume that a nucleus is in thermal equilibrium with a heat bath and particle reservoir or, in TFD terms, in the thermal (phonon) vacuum state. An inelastic collision of a hot nucleus with neutrinos leads to transitions from the thermal vacuum to thermal one-phonon states.

In the derivation of the relevant cross section at finite temperature we follow the formalism by

Walecka–Donnelly [14, 15], which describes in a unified way electromagnetic and weak semileptonic processes by taking advantage of the multipole decomposition of the relevant hadronic current density operator. In the case of neutral-current neutrino–nucleus scattering, the differential cross section for a transition from an initial nuclear state (i) to a final state (f) can be written as a sum over all allowed multipolarities J^π

$$\begin{aligned} \frac{d\sigma_{i \rightarrow f}}{d\Omega} &= \frac{2G^2 (E_\nu - \omega_{if})^2 \cos^2(\theta/2)}{\pi (2J_i + 1)} \\ &\times \left\{ \sum_{J=0}^{\infty} \sigma_{\text{CL}}^J + \sum_{J=1}^{\infty} \sigma_{\text{T}}^J \right\}, \end{aligned} \quad (12)$$

where

$$\sigma_{\text{CL}}^J = \left| \left\langle J_f \left\| \hat{M}_J + \frac{\omega_{if}}{q} \hat{L}_J \right\| J_i \right\rangle \right|^2 \quad (13)$$

and

$$\begin{aligned} \sigma_{\text{T}}^J &= \left(-\frac{q_\mu^2}{2q^2} + \tan^2 \frac{\theta}{2} \right) \\ &\times \left[\left| \left\langle J_f \left\| \hat{J}_J^{\text{mag}} \right\| J_i \right\rangle \right|^2 + \left| \left\langle J_f \left\| \hat{J}_J^{\text{el}} \right\| J_i \right\rangle \right|^2 \right] \\ &- \tan \frac{\theta}{2} \sqrt{-\frac{q_\mu^2}{2q^2} + \tan^2 \frac{\theta}{2}} \\ &\times \left[2\text{Re} \left\langle J_f \left\| \hat{J}_J^{\text{mag}} \right\| J_i \right\rangle \left\langle J_f \left\| \hat{J}_J^{\text{el}} \right\| J_i \right\rangle^* \right]. \end{aligned} \quad (14)$$

Here, G is the electroweak coupling constant, θ is the scattering angle, E_ν is the incoming neutrino energy, ω_{if} is the transition energy from the initial nuclear state (i) to the final state (f), and $q_\mu = (\omega_{if}, \mathbf{q})$

$$\left(q = |\mathbf{q}| = \sqrt{\omega_{if}^2 + 4E_\nu(E_\nu - \omega_{if}) \sin^2 \frac{\theta}{2}} \right)$$

is the four-momentum transfer. The operators \hat{M}_J , \hat{L}_J , \hat{J}_J^{el} , and \hat{J}_J^{mag} are the multipole operators for the charge, longitudinal, and transverse electric and magnetic parts of the four-current, respectively. Following [14] they can be written in terms of one-body operators in the nuclear many-body Hilbert space.

The cross section involves the reduced matrix elements of these operators between the initial and final nuclear states. Within the present approach, the initial nuclear state is the thermal phonon vacuum (TV) and the final states are the thermal one-phonon states. Therefore, at $T \neq 0$ all the reduced matrix elements in Eqs. (13), (14) are calculated in accordance with Eqs. (11). The total cross section is obtained from the differential cross sections by summing over

all possible one-phonon states of different multipolarity and by numerical integration over scattering angles

$$\sigma(E_\nu) = 2\pi \sum_{f \in \{\lambda i\}} \int_1^{-1} \frac{d\sigma_{\text{TV} \rightarrow f}}{d\Omega} d\cos\theta. \quad (15)$$

Up to moderate energies ($E_\nu \sim 15\text{--}20$ MeV), the INNS is dominated by the neutral-channel Gamow–Teller transitions $J^\pi = 1^+$. Moreover, in the $q \rightarrow 0$ limit, the full operator exciting 1^+ states is reduced to the following Gamow–Teller operator:

$$\text{GT}_0 = \left(\frac{g_A}{g_V} \right) \boldsymbol{\sigma} t_0, \quad (16)$$

where $(g_A/g_V) = -1.2599$ [16] is the ratio of the axial and vector weak coupling constants, $\boldsymbol{\sigma}$ is the spin operator and t_0 is the zero component of the isospin operator in spherical coordinates.

To circumvent computational limitations in the LSSM calculations [3–5] the total INNS cross section $\sigma(E_\nu)$ was split into two parts—a down-scattering part $\sigma_d(E_\nu)$ and the up-scattering part $\sigma_u(E_\nu)$. The term $\sigma_d(E_\nu)$ includes transitions where the scattered neutrino loses energy, whereas the term $\sigma_u(E_\nu)$ includes those transitions where the neutrino gains energy from a hot nucleus. Assuming the validity of the Brink hypothesis for the GT_0 resonance, the down-scattering term was transformed to a sum over only those final excited nuclear states which are coupled by a direct GT_0 transition with the nuclear ground state. As a result, $\sigma_d(E_\nu)$ appeared to be independent of T .

In our case, the part $\sigma_d(E_\nu)$ corresponds to transitions from $|0(T); \text{ph}\rangle$ to $|Q_{\lambda i}\rangle$ states with positive energies, whereas the $\sigma_u(E_\nu)$ term is the sum of transitions $|0(T); \text{ph}\rangle \rightarrow |\tilde{Q}_{\lambda i}\rangle$ where the tilde-states have negative energies. In the latter transitions a neutrino gains energy due to nuclear de-excitation.

Thus within the present approach the GT_0 ($J^\pi = 1^+$) contribution to the cross section reads

$$\begin{aligned} \sigma(E_\nu) &= \sigma_d(E_\nu) + \sigma_u(E_\nu) \quad (17) \\ &= \frac{G^2}{\pi} \sum_i (E_\nu - \omega_{J_i})^2 \Phi_{J_i} + \frac{G^2}{\pi} \sum_i (E_\nu + \omega_{J_i})^2 \tilde{\Phi}_{J_i}. \end{aligned}$$

The probabilities Φ_{J_i} and $\tilde{\Phi}_{J_i}$ are given in (11) with $\mathcal{T} = \text{GT}_0$. Since ω_{J_i} , Φ_{J_i} , and $\tilde{\Phi}_{J_i}$ are functions of T , both terms σ_d and σ_u depend on temperature.

Whereas the GT_0 component determines the neutrino–nucleus cross section at low E_ν , higher multipole contributions become increasingly important at higher neutrino energies. Moreover, at higher

neutrino energies Eq. (16) for GT_0 is not valid and the 1^+ -transition operator will depend on transfer momentum q . According to [17, 18] the q dependence reduces the cross section.

3. CALCULATIONS FOR THE HOT NUCLEUS ^{54}Fe

Numerical calculations have been performed for ^{54}Fe . The single-particle wave functions and energies were calculated in a spherically symmetric Woods–Saxon potential. The constants of the pairing interaction were determined to reproduce experimental pairing energies in the BCS approximation. All parameters are the same as in our previous calculations [6, 19] for electron capture rates on the same nucleus at $T \neq 0$.

The radial dependence of the residual multipole and spin-multipole forces is chosen in the form $R_\lambda(r) = \partial U(r)/\partial r$, where $U(r)$ is the central part of the single-particle Woods–Saxon potential. Thus, $R_\lambda(r)$ as well as the parameters $\kappa_{0,1}^{(\lambda)}$ and $\kappa_{0,1}^{(L\lambda)}$ do not depend on λ . The isovector parameters $\kappa_1^{(\lambda)}$ and $\kappa_1^{(L\lambda)}$ are fitted to the experimental position of the $E1$ [20] and $M1$ [21] resonances in ^{54}Fe . According to the estimates in [22, 23], the isoscalar spin-multipole interaction is very weak in comparison with the isovector one. Following [23], we take $\kappa_0^{(L\lambda)}/\kappa_1^{(L\lambda)} = 0.1$.

First, we have performed TQRPA calculations of the GT_0 strength distribution in ^{54}Fe . As in the LSSM calculations [4], the GT_0 operator (16) have been scaled by a quenching factor 0.74. In Fig. 1, we display the GT_0 strength distributions for the ground state ($T = 0$) of ^{54}Fe and at three stellar temperature values, occurring at different collapse stages: $T = 0.86$ MeV corresponds to the condition in the core of a presupernova model for a $15M_\odot$ star; $T = 1.29$ and 1.72 MeV relate approximately to the neutrino trapping and neutrino thermalization stages, respectively. All results are plotted as a function of the energy transfer to ^{54}Fe . For charge-neutral reactions this energy is equal to a thermal phonon energy ω_{J_i} .

At $T = 0$, the transition strength is concentrated mostly in one-phonon 1^+ state forming the GT_0 resonance near $\omega \approx 10$ MeV. The main contribution to the phonon structure comes from the proton and neutron single-particle transitions $1f_{7/2} \rightarrow 1f_{5/2}$. With temperature increase the fraction of low-energy transitions in the GT_0 strength distribution increases. The physical reason is the weakening and subsequent collapse of pairing correlations (at $T \approx 0.8$ MeV) and appearance of low-energy particle–particle and hole–hole transitions due to thermal smearing of neutron

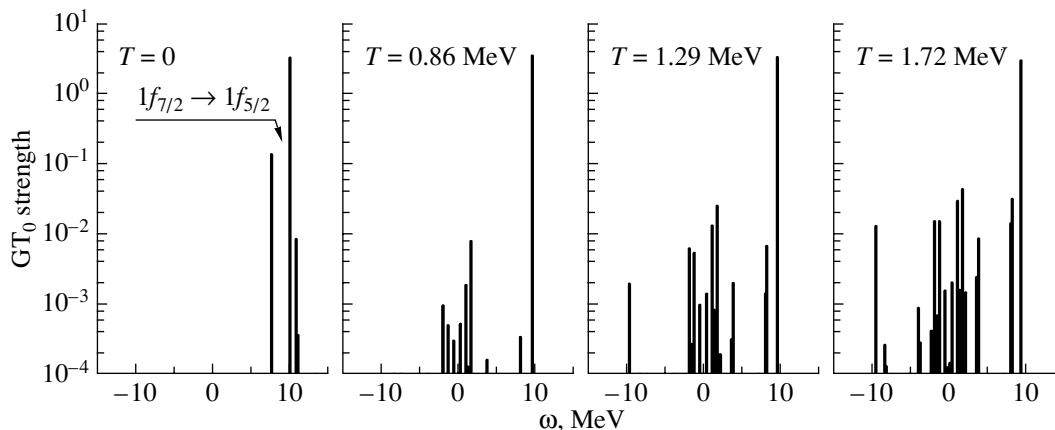


Fig. 1. GT_0 strength distributions in the ^{54}Fe nucleus at different temperatures T as a function of the energy of transition ω .

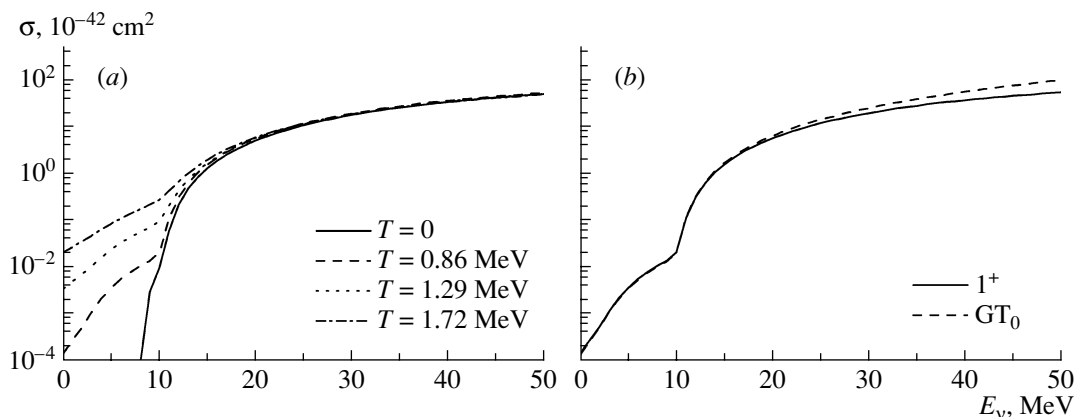


Fig. 2. (a) Contribution of 1^+ transitions to the cross section of neutrino inelastic scattering off ^{54}Fe calculated with the q -dependent 1^+ excitation operator as a function of neutrino energy E_ν at different stellar temperatures T ; (b) A comparison of the cross sections of neutrino inelastic scattering off ^{54}Fe calculated with the q -dependent 1^+ excitation operator (solid curve) and the GT_0 excitation operator (16) (dashed curve) at $T = 0.86$ MeV.

and proton Fermi surfaces. Moreover, at finite temperature the “negative energy” transitions to tilde one-phonon states appear. As a result, the GT_0 energy centroid is shifted down by 1.1 MeV at $T = 1.72$ MeV. This indicates a violation of the Brink hypothesis within the present approach.

The contribution of 1^+ transitions to the INNS cross section is shown in Fig. 2a for different temperatures. The calculations have been performed with the exact q -dependent 1^+ multipole transition operator [14]. As in the LSSM calculations [3], the cross section $\sigma(E_\nu)$ at $T = 0$ is equal to zero when E_ν is less than the energy of the lowest 1^+ state in ^{54}Fe . Within the QRPA, the lowest 1^+ state in ^{54}Fe has an excitation energy of $\omega(1^+) \approx 7.5$ MeV (see Fig. 1). The GT_0 transitions at $T \neq 0$ do not show such a gap due to thermally unblocked low- and negative-energy transitions. As a consequence, there is no threshold energy for neutrinos

at finite temperatures and the INNS cross section appears to be quite sensitive to T at neutrino energies $E_\nu < 10$ MeV. As it follows from the present calculations as well as from the LSSM study [3], thermal effects can increase the low-energy cross section by up to two orders of magnitude when the temperature rises from 0.86 to 1.72 MeV. Finite temperature effects are unimportant for $E_\nu > 15$ MeV where excitation of the GT_0 resonance becomes possible and dominates the cross section. These features were pointed in [3] as well.

To check the influence of finite momentum transfer on the INNS cross section we also have performed calculations with the GT_0 transition operator (16). A comparison of 1^+ and GT_0 cross sections is shown in Fig. 2b for $T = 0.86$ MeV. The q dependence becomes important at $E_\nu > 30$ MeV. At $E_\nu = 35$ MeV the INNS cross section calculated with the q -dependent 1^+ operator is by 20% less than that calculated with

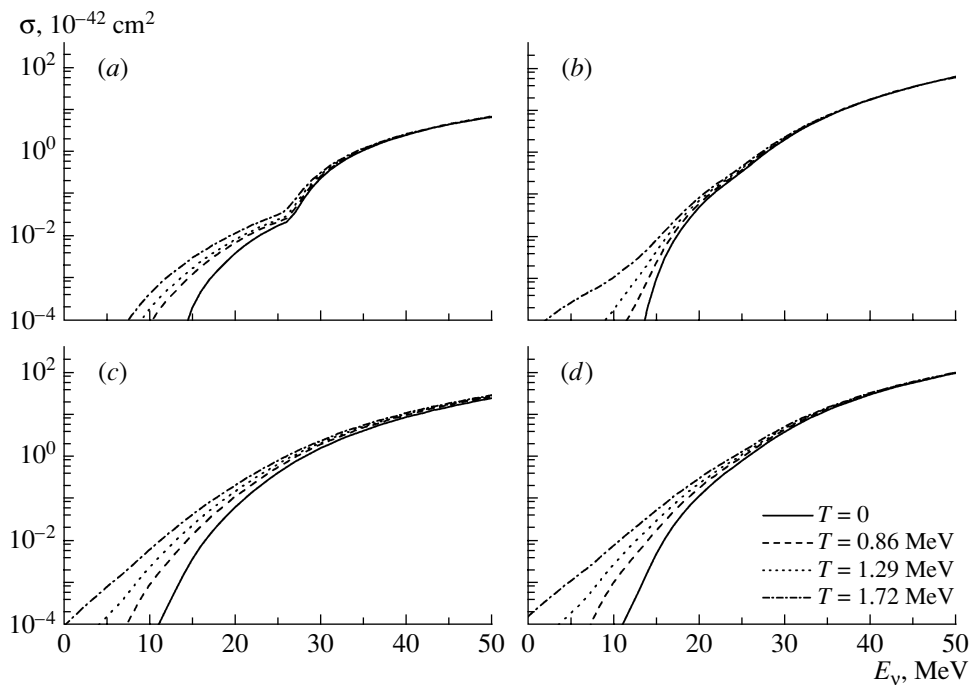


Fig. 3. Contributions of different first-forbidden transitions to the neutrino–nucleus inelastic scattering cross sections for ^{54}Fe at different temperatures T : (a) the contribution of the 0^- transitions; (b) the contribution of the 1^- transitions; (c) the contribution of 2^- transitions; (d) the summed contribution of the all first-forbidden transitions.

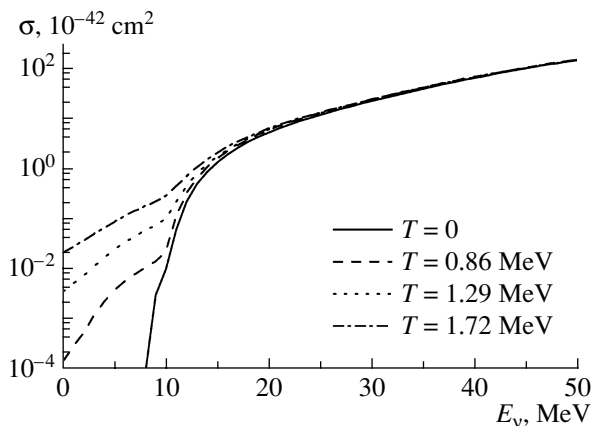


Fig. 4. The neutrino–nucleus inelastic scattering cross sections as the sum of allowed and first-forbidden contributions for ^{54}Fe at different temperatures T .

the GT_0 operator (16). At $E_\nu = 50$ MeV the difference is about factor of 2. The effect does not change with temperature.

The contribution of first-forbidden transitions 0^- , 1^- , and 2^- to the INNS cross section was also calculated within the TQRPA, taking into account the q dependence as given in [14]. The results are presented in Fig. 3. As it can be seen, a temperature increase enhances the cross sections at low and moderate E_ν . The main reason is thermally unblocked

low-energy first-forbidden transitions. According to our calculations 2^- transitions dominate the total contribution of first-forbidden transitions to the cross section at low neutrino energies, while at higher energies the total contribution is mainly determined by the 1^- transitions.

In Fig. 4, the INNS cross sections at different temperatures are shown as a sum of 1^+ , 0^- , 1^- , and 2^- contributions (we omit the contribution of the 0^+ multipole because it is negligible). At low E_ν the cross sections are almost completely dominated by the GT_0 transitions. The part of the cross sections arising from the first-forbidden transitions becomes increasingly important at larger E_ν . We find that for $E_\nu = 30$ MeV up to 20% of the cross section is due to first-forbidden transitions. For $E_\nu = 40$ MeV allowed and forbidden transitions contribute about equally, while at $E_\nu = 50$ MeV the contribution of first-forbidden transitions is nearly twice as large as that of 1^+ transitions.

In the LSSM calculations, the temperature-related enhancement of $\sigma(E_\nu)$ was only due to the neutrino up-scattering. In our approach both the up-scattering and down-scattering parts of $\sigma(E_\nu)$ are temperature dependent. To analyze the relative importance of these two types of scattering processes we display them separately as the functions of E_ν for different values of T in Fig. 5.

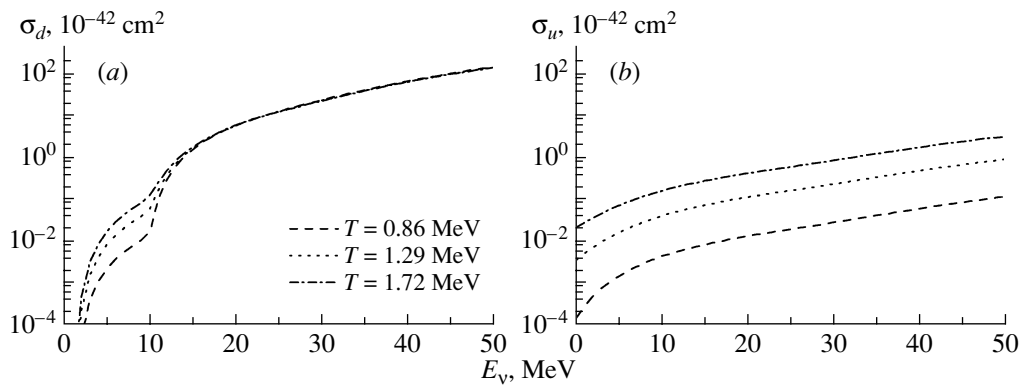


Fig. 5. The down-scattering $\sigma_d(E_\nu)$ (a) and the up-scattering $\sigma_u(E_\nu)$ (b) parts of the neutrino–nucleus inelastic scattering cross section for ^{54}Fe at different T .

A weak T dependence of σ_d is seen at low neutrino energies $E_\nu < 12$ MeV. At higher energies σ_d practically does not depend on T . As the function of E_ν the down-scattering cross section sharply increases at low neutrino energies and then grows more slowly. Instead, σ_u is quite sensitive to temperature but its dependence on E_ν is obviously smoother than that of σ_d (at least at $E_\nu < 15$ MeV). The absolute values of σ_d and σ_u are of the same order of magnitude only at quite low neutrino energies $E_\nu \lesssim 4\text{--}10$ MeV.

Thus the conclusion is that the T dependence of the INNS cross section at low neutrino energies is mainly due to up-scattering process, whereas at neutrino energies $E_\nu > 15$ MeV, when the thermal effects are much less important, the INNS cross section is determined by the neutrino down-scattering.

The above conclusions agree well with the results of the LSSM studies for even–even nuclei [3, 4]. Furthermore, our results for σ_d confirm the applicability of approximations based on the Brink hypothesis, which has been used in calculations of σ_d in the LSSM.

4. CONCLUSIONS

We have performed studies of the temperature dependence of the cross section for inelastic neutrino–nucleus scattering off the hot nucleus ^{54}Fe . Thermal effects were treated within the thermal quasiparticle random-phase approximation in the context of the TFD formalism. These studies are relevant for supernova simulations.

In contrast to the large-scale shell-model studies [3, 4] we do not assume the Brink hypothesis when treating the down-scattering component of the cross section $\sigma(E_\nu)$. Moreover, we take into account thermal effects not only for the allowed 1^+ transitions but also for the first-forbidden transitions 0^- , 1^- , and 2^- . For all multipole contributions we have performed

the calculations with momentum dependent multipole operators.

Despite these differences between the two approaches, our calculations have revealed the same thermal effects as were found in [3, 4]: A temperature increase leads to a considerable enhance of the INNS cross section for neutrino energies lower than the energy of the GT_0 resonance. This enhancement is mainly due to neutrino up-scattering at finite temperature. The calculated cross sections for ^{54}Fe are very close to those given in [4]. Thus, the results of our study show that the present approach provides a valuable tool for the evaluation of the inelastic neutrino–nucleus cross sections under stellar conditions. The approach can be easily adopted to calculate the INNS cross sections as a function of scattering angle.

ACKNOWLEDGMENTS

The fruitful discussions with K. Langanke and G. Martínez-Pinedo are gratefully acknowledged. This work is supported in part by the Heisenberg–Landau Program and the DFG grant (SFB 634).

REFERENCES

1. W. C. Haxton, Phys. Rev. Lett. **60**, 1999 (1988).
2. G. M. Fuller and B. S. Meyer, Astrophys. J. **376**, 701 (1991).
3. J. M. Sampaio et al., Phys. Lett. B **529**, 19 (2002).
4. A. Juodagalvis et al., Nucl. Phys. A **747**, 87 (2005).
5. K. Langanke et al., Phys. Rev. Lett. **100**, 011101 (2008).
6. A. A. Dzhiyev et al., Phys. Rev. C **81**, 015804 (2010).
7. Y. Takahashi and H. Umezawa, Collect. Phenom. **2**, 55 (1975).
8. H. Umezawa, H. Matsumoto, and M. Tachiki, *Thermo Field Dynamics and Condensed States* (North-Holland, Amsterdam, 1982).
9. I. Ojima, Ann. Phys. (N.Y.) **137**, 1 (1981).

10. T. Hatsuda, Nucl. Phys. A **492**, 187 (1989).
11. A. A. Dzhioev and A. I. Vdovin, Int. J. Mod. Phys. E **18**, 1535 (2009).
12. A. I. Vdovin and A. A. Dzhioev, Phys. Part. Nucl. **41**, 1127 (2010).
13. V. G. Soloviev, *Theory of Atomic Nuclei: Quasi-particle and Phonons* (Inst. Phys. Publ., Bristol, Philadelphia, 1992).
14. J. D. Walecka, in *Muon Physics*, Vol. 2, Ed. by V. W. Hughes and C. S. Wu (Academic Press, New York, 1975), p. 113.
15. T. W. Donnelly and R. D. Peccei, Phys. Rep. **50**, 1 (1979).
16. I. S. Towner and J. C. Hardy, in *Symmetries and Fundamental Interactions in Nuclei*, Ed. by W. C. Haxton and E. M. Henley (World Sci., Singapore, 1995), p. 183.
17. E. Kolbe et al., Phys. Rev. C **60**, 052801 (1999).
18. A. Hektor et al., Phys. Rev. C **61**, 055803 (2000).
19. A. A. Dzhioev et al., Bull. RAS, Phys. **72**, 269 (2008).
20. J. W. Norbury et al., Aust. J. Phys. **31**, 471 (1978).
21. D. I. Sober et al., Phys. Rev. C **31**, 2054 (1985).
22. Dao Tien Khoa et al., Preprint №E4-86-198, JINR (Dubna, 1986).
23. V. Ponomarev et al., J. Phys. G **13**, 1523 (1987).